# Investigation of Indoor Atmospheric Attenuation on Visible Light Positioning for Industrial Applications

Vinson Javiero, Muhammad Ijaz, Sunday Ekpo, Chen Chen, Mohammad-Ali Khalighi, Bamidele Adebisi

# Investigation of Indoor Atmospheric Attenuation on Visible Light Positioning for Industrial Applications


Vinson Javiero
*Manchester Metropolitan University*
*School of Engineering*
Manchester, United Kingdom
vinson.javiero@stu.mmu.ac.uk

Muhammad Ijaz
*Manchester Metropolitan University*
*School of Engineering*
Manchester, United Kingdom
m.ijaz@mmu.ac.uk

Sunday Ekpo
*Manchester Metropolitan University*
*School of Engineering*
Manchester, United Kingdom
s.ekpo@mmu.ac.uk

Chen Chen
*School of Microelectronics and Communication Engineering*
*Chongqing University*
China
c.chen@cqu.edu.cn

Mohammad-Ali Khalighi
*Centrale Marseille, Institut Fresnel*
Marseille, France
ali.khalighi@fresnel.fr

Bamidele Adebisi
*Manchester Metropolitan University*
*School of Engineering*
Manchester, United Kingdom
b.adebisi@mmu.ac.uk



***Abstract*— In the past decade, visible light communication (VLC) technology has received increasing attention for numerous applications, including for indoor visible light positioning (VLP). The transmission medium for indoor VLP systems in industrial environments could include smoke particles, oil vapors, water mist, and industrial fumes. This work investigates the indoor atmospheric attenuation on the performance of VLP for industrial scenarios. The considered VLP technique uses trilateration based on the Cayley-Menger-Determinant algorithm. The positioning method uses optical received signal strength (RSS) to estimate a drone's position. Smoke and fog effects for the indoor atmospheric attenuations have been considered for visibility (*V*) ranging from 15 m to 1 km. The results show that the position error increases from an average value of 5.73 cm in clear air to 28.41 cm and 29.94 cm with smoke and fog attenuation, respectively. Indeed, there is a slightly higher received power in the presence of smoke, as compared to fog, for a given visibility range.**



***Keywords*— Indoor Localization, Indoor Positioning, Industrial Environment, Visible Light Positioning, Atmospheric Attenuation.**


## I. INTRODUCTION

Unmanned Aerial Vehicles (UAVs), popularly known as drones, are utilized for a variety of purposes for indoor industrial applications, including automated autonomous operations. Drones are primarily used to conduct visual inspections in a variety of indoor and outdoor situations because they provide a safe and cost-effective solution to inspect hard-to-reach areas and inspect different heights [1]. Offshore oilrigs, power plants, facades, controlling physical stock-taking in warehouses, and spreading farm animal feed across broad areas are some of the areas of potential applications for drones using VLP. UAVs can also be used to investigate piping systems within the buildings for detecting damages or leakages. The fundamental challenge, however, is that the drone must precisely detect its location concerning its surroundings.

A few recent works have tackled this problem by using an indoor positioning system based on different technologies such as blue light-wavelength [2], and VLC transmitters and receivers [3]. As light-emitting-diode (LED) based infrastructure is readily available in most buildings and industrial locations. VLP offers a huge possibility for indoor localization and tracking of drones. VLP also allows for license-free operation with no electromagnetic interference. Localization based on VLP has already been deployed in supermarkets and shown with a drone built by Philips Lighting [4].

A lot of research has been done on the development and performance improvement of VLC systems over the last decade [5] However, there has been limited work in the literature examining the performance of VLC systems in industrial environments.

Most VLC-based indoor localization systems are designed for two-dimensional (2D) positioning to calculate (x,y) coordinates, and three-dimensional (3D) positioning, assuming clear air conditions. This assumption is not always valid in industrial environments. Oil vapour, water mist, industrial fumes, or even coal particles can all contribute to signal attenuation, depending on the sort of industrial setting. These particles can cause light signal attenuation and scattering which leads to VLP positioning errors [6]. To the best of authors' knowledge, there is no existing work that investigates the impact on the received power and VLP accuracy of a UAV flight path due to indoor atmospheric attenuations [7].

In this paper, we investigate the positioning accuracy of VLP with and without atmospheric attenuation in industrial applications. Both shot and thermal noises are considered, which are modelled as additive white Gaussian (AWGN). VLP is achieved using a trilateration indoor positioning based on the Cayley-Menger-Determinant (CMD) algorithm like our previous work in [8]. The positioning method uses optical received signal strength (RSS), and a blue filter is used at the receiver to limit the background noise effect [9]. Smoke and fog effects for the indoor atmospheric attenuations have been considered for visibility (*V*) ranging from 15 m to 1 km. The results show that the position error increases from an average value of 5.73 cm in clear air environment to 28.41 cm and 29.94 cm with smoke and fog attenuation, respectively.

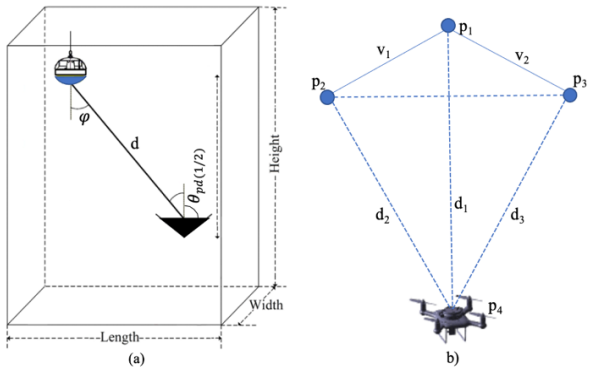


Figure 1: a) The overview of the room's cross-section and b) the schematic diagram for the trilateration problem and its parameters.

The remainder of the paper is organized as follows: Section II outlines the system model, the theory on fog and smoke attenuation and the CMD algorithm. In Section III, simulation results and discussion are presented. Conclusions are finally drawn in Section V.

## II. System Model

Figure 1 shows the schematic of the considered system. It consists of a typical industrial environment (25m × 15m × 5m) with 15 uniformly distributed light fixtures on the ceiling with 5m spacing per transmitter. Each light fixture has a half semi-angle of 60° and a power of 80 Watts, strong output luminaires being typical in industrial environments [10]. The main simulation parameters are shown in Table 1.

The $N$ light fixtures are placed at a fixed height $h_{LED}$ with coordinates $(x_i, y_i, h_{LED})$ $i = 1 \dots N$. The receiver, with a photodetector (PD) area $A_{pd}$ is located at the unknown location $(x, y, z)$. For typical LEDs with Lambertian radiation pattern $m$, the received power $P_{ri}$ from $i^{\text{th}}$ transmitter is given by [11]:

$$P_{ri} = \begin{cases} P_{ti} \frac{(m+1)A_{pd}}{2\pi d_i^2} \cos^m(\varphi) \cos(\psi), & \psi \le \theta_{pd} \\ 0, & \psi > \theta_{pd} \end{cases} \quad (1)$$

where $P_{ti}$ is the transmitter power, $d_i$ is the distance between the transmitter and the receiver, $\varphi$ is the angle of irradiance, $\psi$ is the angle of incidence, and $\theta_{pd}$ is the field of view of the receiver, as shown in Fig.1 (a).

The effect of smoke and fog attenuation has been considered in (1) using the laboratory-based smoke and fog model and the $q$ values proposed are showed in [12] and is given by:

$$\beta_\lambda\,(dB/km) = \frac{17}{V(km)} \left(\frac{\lambda}{\lambda_0}\right)^{-q(\lambda)} \quad (2)$$

$$q(\lambda) = \begin{cases} 0.1428\lambda - 0.0947 & Fog \\ 0.8467\lambda - 0.5212 & Smoke \end{cases} \quad (3)$$

The distance between the transmitter and the receiver $d_i$ can be calculated from the received signal power, $P_{ri}$. Moreover, given $\cos(\varphi) = \cos(\psi) = \frac{h_{LED} - z}{d_i} = \frac{\Delta h}{d_i}$ for horizontally oriented transmitters and receiver, the estimated distance $\widehat{d}_i$ can be calculated as [13]:

$$\widehat{d}_i = \sqrt[m+3]{\frac{(m+1)\,A_{pd}\,P_t\,\Delta h^{m+1}}{2\,\pi\,P_{ri}}} \quad (4)$$

where $\Delta h = h_{LED} - z$ is the unknown vertical height difference between the transmitter and the receiver. Note that, the estimated distance $\widehat{d}_i$ cannot be directly calculated from $P_{ri}$ without knowing the accurate $\Delta h$. Due to this, we generate a set of estimated distances $\widehat{d}_i$ for different possible heights $h$ should be z ranging from 0 m ($h_{min}$) to $h_{LED}$ with height resolution $R_h$ of $1\,mm$. This leads to the accurate estimation of $\widehat{d}_i$. The received signal is affected by shot and thermal noises with the total variance $\sigma^2_{noise} = \sigma^2_{shot} + \sigma^2_{thermal}$. The signal-to-noise (SNR) ratio can be calculated using:

$$\mathrm{SNR}_i(\mathrm{dB}) = 10\log_{10} \frac{(R_r P_{ri})^2}{\sigma^2_{noise}} \quad (5)$$

where $R_r$ is the receiver's PD responsivity.

TABLE I
Simulation Parameters

| Parameter | Value |
|---|---|
| Width × Length × Height | 25 m × 15 m × 5 m |
| Transmitter's Power - $P_t$ | 80 W |
| Transmitter's semi-angle $\varphi$ | 60° |
| Receiver's Height | 0 – 3.6 m |
| Photodetector Area - $A_{pd}$ | 1 cm$^2$ |
| Receiver's FOV (half angle) - $\theta_{pd(1/2)}$ | 80° |
| Receiver's Responsivity - $R_r$ | 0.54 A/W |
| Bandwidth | 10 MHz |
| Visibility for fog and smoke | 0.015 km- 1 km |
| Optical Filter | 450 nm |

### A. Positioning Algorithm

Then, the positioning algorithm is performed for each of the sets of generated distances $\widehat{d}_i$ (i=1..N) at different heights using (4). Fig. 1. b shows the three transmitters *p1*, *p2*, and *p3* positions and with *p4* being the unknown drone location. The algorithm only requires three transmitter positions, meaning that the corresponding signals from the three nearest (i.e. strongest) LEDs are taken into account, as they offer the highest SNR.

The Cayley-Menger bideterminant of two sequences of $n$ points $[p_1, p_2, \cdots, p_n]$ and $[q_1, q_2, \cdots, q_n]$ is defined as [14]:

$$D(p_1, \dots, p_n;\, q_1, \dots, q_n) = 2\left(\frac{-1}{2}\right)^n \begin{vmatrix} 0 & 1 & 1 & 1 & 1 \\ 1 & D(p_1,q_1) & D(p_1,q_2) & \cdots & D(p_1,q_n) \\ 1 & D(p_2,q_1) & D(p_2,q_2) & \cdots & D(p_2,q_n) \\ \vdots & \vdots & \vdots & \ddots & \vdots \\ 1 & D(p_n,q_1) & D(p_n,q_2) & \cdots & D(p_n,q_n) \end{vmatrix} \quad (6)$$

where $D(p_i; q_j)$ is the squared distance between points $p_i$ and $p_j$. When two sequences of points are the same, then $D(p_1, \dots, p_n;\, q_1, \dots, q_n)$ is denoted by $D(p_1, \dots, p_n)$ and

CMD is given by:

$$D(p_1,p_2,p_3,p_4) = \frac{1}{8}\begin{vmatrix} 0 & 1 & 1 & 1 & 1 \\ 1 & 0 & D(p_1,p_2) & D(p_1,p_3) & D(p_1,p_4) \\ 1 & D(p_2,p_1) & 0 & D(p_2,p_3) & D(p_2,p_4) \\ 1 & D(p_3,p_1) & D(p_3,p_2) & 0 & D(p_3,p_4) \\ 1 & D(p_4,p_1) & D(p_4,p_2) & D(p_4,p_3) & 0 \end{vmatrix} \quad (7)$$

where $p_4$ is the location of the drone, meaning that $D(p_4,p_1), D(p_4,p_2), D(p_4,p_3)$ are distances $\widehat{d_1}$, $\widehat{d_2}$, $\widehat{d_3}$ that are computed from the received power measurements. It is possible to calculate the position of the receiver $(p_4)$ with respect to three known transmitter coordinates $(p_1,p_2,p_3)$ using:

$$p_4 = p_1 + k_1 v_1 + k_2 v_2 \pm k_3 (v_1 v_2) \quad (8)$$

where $v_1 = p_2 + p_1$ and $v_2 = p_3 - p_1$, and

$$k_1 = -\frac{D(p_1,p_2,p_3;p_1,p_3,p_4)}{D(p_1,p_2,p_3)},$$

$$k_2 = \frac{D(p_1,p_2,p_3;p_1,p_2,p_4)}{D(p_1,p_2,p_3)},$$

$$k_3 = \frac{\sqrt{D(p_1,p_2,p_3,p_4)}}{D(p_1,p_2,p_3)}$$

This results in a single estimate $p_4 = (\hat{x},\hat{y},\hat{z})$ for each of the heights.

### B. Cost Function

Once all possible locations have been generated, the estimated location is found at the minimum of *C(h)*, with *C(h)* being the average squared error between the estimated distances $\widehat{d_i}$ calculated using (4), and the distances of the estimated location $(\hat{x},\hat{y},\hat{z})$ from (8). The cost function finds the minima at the receiver's actual height, given by:

$$C(h) = \frac{1}{N}\sum_{i=1}^{N}\left[\widehat{d_i} - \sqrt{(\hat{x}-x_i)^2 + (\hat{y}-y_i)^2 + (\hat{z}-z_i)^2}\right]^2 \quad (9)$$

where $z_i = h_{LED}$.

Using the presented algorithm, the $(x,y,z)$ coordinates of the receiver can be estimated. After calculating the position, the estimated position is compared with the actual position to find the positioning error, given by:

$$D_{error} = \sqrt{(\hat{x}-x)^2 + (\hat{y}-y)^2 + (\hat{z}-z)^2} \quad (10)$$

## III. Results and Discussion

In this section, we present our simulation results in terms of RSS and positioning errors with and without smoke and fog attenuations. The peak received power, $P_r$ with the presence of both smoke and fog attenuation is approximately 5.9 times smaller compared to the received power without indoor attenuation, see Fig. 2. Using equations (1-2), the attenuations co-efficient, $\beta_\lambda$ for the indoor attenuation are 0.16 dB/km for smoke and 0.17 dB/km for fog for *V* ranging from 0.015 - 1 km. Using equation (1), the received power is calculated for all 30 drone positions as shown in Fig. 3 and the results for the $P_r$ are shown in Fig. 2. The average peak received power is $7.81 \times 10^{-5}\ W$ for both smoke and fog, whereas the average received power without indoor attenuation is approximately $1.31 \times 10^{-5}\ W$, see Fig.2.

Figure 3 shows the selected real flight path using a set of 30 positioning samples ranging from 0.1- 3.6 m in height along the industrial warehouse with locations of the transmitter is also provided. Notice, that the estimated path of the drone is very close to the real flight path in the presence of the AWGN noise. However, the estimated path for the drone in the presence of fog and smoke attenuation is not identical to the real path, see inset Fig 3. This is because of smoke and fog attenuation ranging from 0.015 km to 1 km.

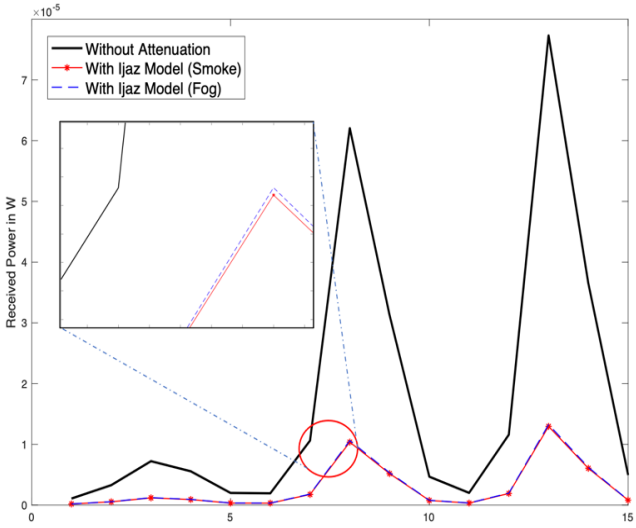


Figure 2: Comparison of received power, $P_r$ without attenuation and with for and smoke attenuation.

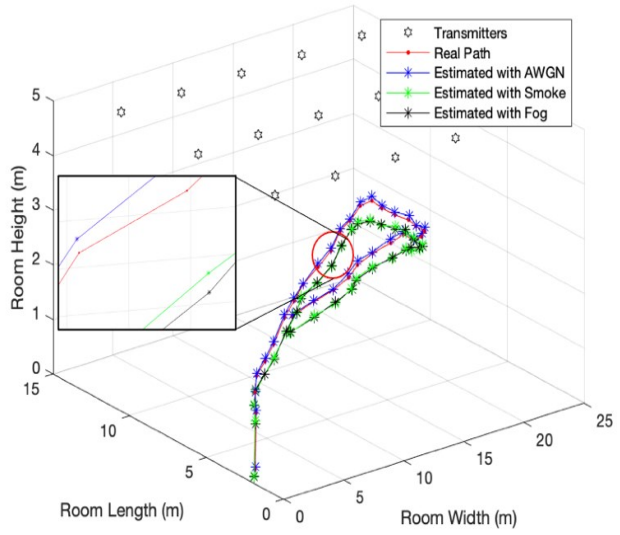


Figure 3: Selected real flight path and comparison with estimated path with AWGN, smoke and fog indoor attenuations.

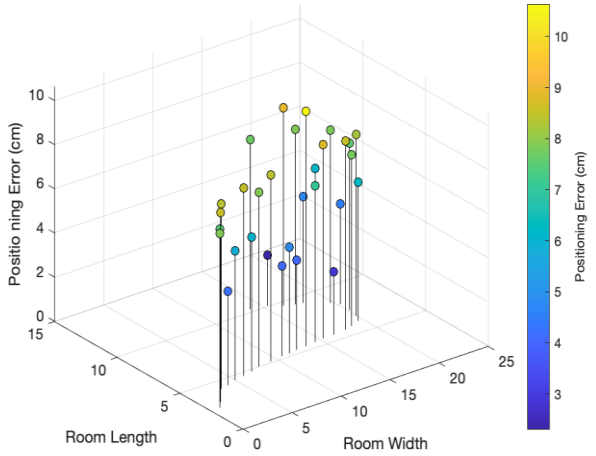


Figure 4: Positioning error in the presence of AWGN and without indoor atmospheric attenuation.

Figure 4 shows the positioning errors in the presence of AWGN noise and without the effect of smoke and fog attenuation. The results show that the estimated positioning errors are 3.8 cm to 9.4 cm and are in good agreement with the real flight path. The average position error was 5.73 cm without considering the atmospheric attention. This accuracy of estimation of the positioning is due to the availability of high SNR without the effect of attenuation.

Figure 5 shows the estimated position error in the presence of smoke actuation for $V$ = 0.015 - 1 km. The smoke attenuation is considered using (2). The estimated positioning error is increased from an average value for the selected path from 5.73 cm to 28.41 cm. Furthermore, the estimated positioning error was ranging from 25.1 cm to 39 cm in the presence of smoke attenuation. Notice that due to the attenuation of the smoke particles when the $V$ reduces that could have an adverse effect on the accuracy of the VLP system due to the high attenuation of the transmit power, see Fig. 2.

The estimated positioning error in the presence of fog actuation for $V$ = 0.015 - 1 km is shown in Fig. 6. The fog attenuation is considered using (2). The estimated positioning error is increased from an average value for the selected path from 5.73 cm to 29.94 cm. Furthermore, the estimated positioning error was ranging from 24 cm to 40 cm in the presence of fog attenuation. Notice that the positioning error is slightly higher due to fog attenuation or water-based vapors in industrial environments than in smoke or dry particles. This could result in higher positioning error and influence the accuracy of the VLP system due to the high attenuation of transmit power, see Fig.2.

## IV. Conclusion

This paper investigates the indoor atmospheric attenuation on the performance of the VLP for industrial applications. The VLP is achieved using a trilateration indoor positioning based on the Cayley-Menger-Determinant (CMD). The positioning method uses optical received signal strength (RSS) to estimate the drone's position with and without the -

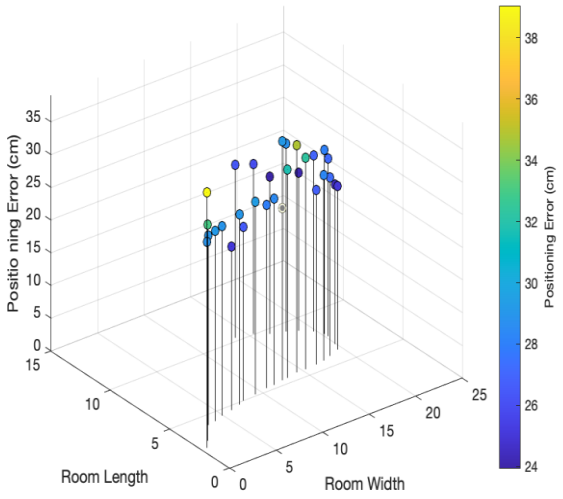


Figure 5: Estimated positioning errors with smoke attenuation for $V$ = 0.015 - 1km.

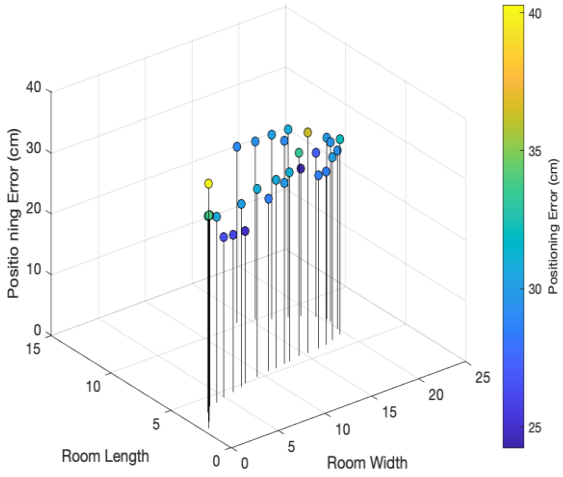


Figure 6: Estimated positioning errors with fog attenuation for $V$ = 0.015 – 1 km.

presence of indoor atmospheric attenuations. Smoke and fog effects for the indoor atmospheric attenuations have been considered for $V$ ranging from 0.015 km to 1 km. The results show that the position error increases from an average value of 5.73 cm without smoke and fog attenuation to 28.41 cm and 29.94 cm with smoke and fog attenuation. It is also noticed that the positioning error is slightly higher due to fog attenuation or water-based vapors in industrial environments than in smoke or dry particles. This could result in an adverse effect on the accuracy of the VLP due to the high attenuation of transmit power.

## References

[1] S. Omari, P. Gohl, M. Burri, M. Achtelik and R. Siegwart, "Visual industrial inspection using aerial robots," Proceedings of the 2014 3rd International Conference on Applied Robotics for the Power Industry, 2014, pp. 1-5, DOI: 10.1109/CARPI.2014.7030056.

[2] Q. Pan, S. Li, S. Liang and Z. Xu, "Blue LD-Based White Light Source for Joint Lighting and Visible Light Communication," 2017 Asia Communications and Photonics Conference (ACP), 2017, pp. 1-3.

[3] M. Kowalczyk and J. Siuzdak, "VLC link with LEDs used as both transmitters and photo-detectors," 2015 Seventh International Conference on Ubiquitous and Future Networks, 2015, pp. 893-897, DOI: 10.1109/ICUFN.2015.7182673.

[4] Philips. Indoor positioning Perfect light, precise location. Available: http://www.lighting.philips.co.uk/systems/lighting-systems/indoor-positioning.

[5] Z. Ghassemlooy, L. N. Alves, S. Zv`anovec, and M. A. Khalighi, Eds., Visible Light Communications: Theory and Applications. CRC-Press, 2017

[6] G. Zachár, G. Vakulya and G. Simon, "Design of a VLC-based beaconing infrastructure for indoor localization applications," 2017 IEEE International Instrumentation and Measurement Technology Conference (I2MTC), 2017, pp. 1-6, DOI: 10.1109/I2MTC.2017.7969837.

[7] Almadani, Y.; Plets, D.; Bastiaens, S.; Joseph, W.; Ijaz, M.; Ghassemlooy, Z.; Rajbhandari, S. Visible Light Communications for Industrial Applications Challenges and Potentials. Electronics 2020, 9, 2157.Mahmoud, A.A.; Ahmad, Z.; Onyekpe, U.; Almadani, Y.; Ijaz, M.; Haas, O.C.L.; Rajbhandari, S. Vehicular Visible Light Positioning Using Receiver Diversity with Machine Learning. Electronics2021,10,3023.

[8] Almadani, Y.; Ijaz, M.; Joseph, W.; Bastiaens, S.; Rajbhandari, S.; Adebisi, B.; Plets, D. A Novel 3D Visible Light Positioning Method Using Received Signal Strength for Industrial Applications. *Electronics* **2019**, *8*, 1311. https://doi.org/10.3390/electronics8111311.

[9] K. R. Shailesh, "Energy-efficient LED lighting design for horticulture," 2019 1st International Conference on Advanced Technologies in Intelligent Control, Environment, Computing & Communication Engineering (ICATIECE), 2019, pp. 339-342, DOI: 10.1109/ICATIECE45860.2019.9063621.

[10] D. Plets, A. Eryildirim, S. Bastiaens, N. Stevens, L. Martens, and W. Joseph, "A Performance Comparison of Different Cost Functions for RSS-Based Visible Light Positioning Under the Presence of Reflections," in Proceedings of the 4th ACM Workshop on Visible Light Communication Systems, 2017, pp. 37-41: ACM.

[11] D. Plets, S. Bastiaens, N. Stevens, L. Martens, and W. Joseph, "Monte-Carlo Simulation of the Impact of LED Power Uncertainty on Visible Light Positioning Accuracy," in 2018 11th International Symposium on Communication Systems, Networks & Digital Signal Processing (CSNDSP), 2018, pp. 1-6.

[12] M. Ijaz, Z. Ghassemlooy, J. Pesek, O. Fiser, H. Le Minh and E. Bentley, "Modeling of Fog and Smoke Attenuation in Free Space Optical Communications Link Under Controlled Laboratory Conditions," in Journal of Lightwave Technology, vol. 31, no. 11, pp. 1720-1726, June1, 2013, DOI: 10.1109/JLT.2013.2257683

[13] D. Plets, A. Eryildirim, S. Bastiaens, N. Stevens, L. Martens, and W. Joseph, "A Performance Comparison of Different Cost Functions for RSS-Based Visible Light Positioning Under the Presence of Reflections," in *Proceedings of the 4th ACM Workshop on Visible Light Communication Systems*, 2017, pp. 37-41: ACM.

[14] F. Thomas and L. Ros, "Revisiting trilateration for robot localization," *IEEE Transactions on Robotics,* vol. 21, no. 1, pp. 93-101, 2005.